Lasers in Manufacturing Conference 2023

Femtosecond laser ablation of titanium foils in liquid environments

Christian R. Günther[a,*], Philipp L. Maack[a], Jan S. Hoppius[b], Cemal Esen[a], Andreas Ostendorf[a]

[a]*Applied Laser Technologies, Ruhr University Bochum, 44801 Bochum, Germany*
[b]*Lidrotec GmbH, Lothringer Allee 2, 44805 Bochum, Germany*

Abstract

The increased demand of high-tech components with smaller structures and advanced materials is pushing ultrashort laser ablation processes to their limits. Thermal stress and debris are typical defects when exceeding stable process parameters. A key to overcome these limitations will be the transfer of the process from gaseous to liquid environments. The much more efficient heat transfer reduces the heat affected zone and recondensation of ablated matter on the material's surface is prevented. As a result, a clean surface is achieved, and even brittle materials can be processed with a high energy input. In this study, the ablation rate, surface roughness and surface oxidation for titanium foils in both liquid and gaseous environment, are presented and compared respectively. The evaluation is based on scanning electron microscopy, laser scanning microscopy, micro-Raman spectroscopy and energy-dispersive X-ray spectroscopy.

Keywords: laser ablation; ablation rate; surface roughness; Raman spectroscopy; EDX

1. Introduction

High-tech components with small structures challenge the current processes in laser ablation. Thermal effects and recondensation of ablated matter are typical defects when exceeding stable process parameters (Barthels and Reininghaus 2018). To step beyond limitations in micromachining new developments are needed since current processes have already been pushed to their limits (Vorobyev et al. 2006; Bauer et al. 2015). In this study the change of the medium surrounding the ablation process is investigated, comparing the ablation process in gaseous environment and flowing water. It was shown in this

* Corresponding author.

work that laser ablation in liquids improves several parameters to further expand the process window to processing with higher energies, which has already been observed before (Butkus et al. 2019). Main features are the increased heat transfer between surface and medium leading to reduced thermal stress. As a result, even brittle materials can be processed and the surface quality in the ablated area increases. Debris is removed before it can recondense on the surface, which leads to a further quality improvement and additional cleaning steps are not required after processing.

2. Experimental Setup and material

The laser used in this study is a JENOPTIK JenLas D2.fs. The wavelength $\lambda_0 = 1030$ nm, pulse frequency $f_{pulse} = 200$ kHz and pulse duration $t_{pulse} = 400$ fs remain unchanged during all experiments. The average power at the target is set between $P_{avg} = 0.1$ W to 2.4 W for the different investigations. The beam is guided over an area of 200 µm x 200 µm on the target with a Scanlab SCANcube III *10* galvanometer scanner, focused with a non-telecentric f-theta corrected lens of $f = 63$ mm focal length.

The spot size of the laser beam is both calculated and measured to ensure accurate knowledge of the fluence. The calculation of the spot size was carried out in consideration of the changing refractive indices at the transition from gas, glass, and water. Nevertheless, determining the spot radius by measurements was indispensable. Nonlinear effects in the liquid can lead to changes that are hard to control. Those effects can lead to self-focusing and filamentation of the beam in dense media (Kanitz et al. 2019). As a result, the beam path can be different to the beam propagation described by e.g., Snell's law. So, another method was used to determine the spot size, which has been introduced by J.M. Liu (Liu 1982).Since this method is based on the measurement of ablated spots the beam propagation must not exactly be verifiable, which is one of the main advantages using this method. The occurring non-linear effects in water are depending on the energy density of the laser beam, leading to different spot sizes with changing laser power. Considering those effects two different spot sizes were used for processing in water and one spot size for processing in argon (table 1).

Table 1. Parameters for the experiments: Fluence, corresponding spot size and scanning speed

Medium	Fluence	Radius focal point	Scanning Speed:
Argon	0 – 3.0 Jcm^{-2}	10.03 µm	10, 20, …, 150 $mm\,s^{-1}$
Water	0 – 0.7 Jcm^{-2} 0.7 – 7 Jcm^{-2}	10.77 µm 6.58 µm	10, 20, …, 150 $mm\,s^{-1}$

The material used in the experiment is a grade 1 titanium foil of 125 µm thickness. For the ablation process the titanium foil sticks on a polymer, which in turn is held in place by a vacuum chuck. The chuck secures the foil in place to precisely keep its position during the entire process (shown in figure 1). In addition, this method ensures a uniform distance between foil and scanner head at all positions.

For processing in gaseous environment argon was chosen since it is commonly used to ensure an inert environment. Using a 1 mm x 12 mm nozzle a constant flow of 25 $l\,min^{-1}$ was applied on the samples surface. For processing in flowing liquid deionized water (electric conductivity of $\sigma \approx 3$ $\mu S\,cm^{-1}$) was used. In contrary to the argon flow the process was kept in a chamber to carefully adjust the characteristics of the water flow. A custom-made chamber was built to be in control of the waterflow and prevent unexpected effects like a changing thickness of the water layer. The chamber, which is shown in figure 1, provides a uniform layer of flowing water at a speed of $v < 1\,m\,s^{-1}$, which was kept constant during all experiments.

The parameters for the experiments were chosen to improve comparability between processing in argon and processing in water. The same parameters could not be used for both media. Especially the high energy

input, that is used for processing in a liquid environment, is not tolerated by the material when processing in gaseous environment. A pre-study led to the parameters shown in table 1, ensuring similar ablation depth, resulting in good comparability of the two processes. In exception of the laser power all laser parameters remained unchanged during the experiments.

For measuring the surface roughness and ablation depth an *Olympus LEXT 3D Measuring Laser Microscope OLS5000-SAF* with an *LMPlanFL N 50x* objective was used. Energy dispersive X-ray spectroscopy (EDX) measurements were performed with a *ZEISS EVO MA 10* Scanning electron microscope (SEM) and a *Bruker Quantax XFlash Detector 410-M*. The SEM was also used to obtain the images. Raman measurements were performed with a *Renishaw inVia* Raman microscope (50x objective, excitation wavelength 532 nm and 33 mW laser power).

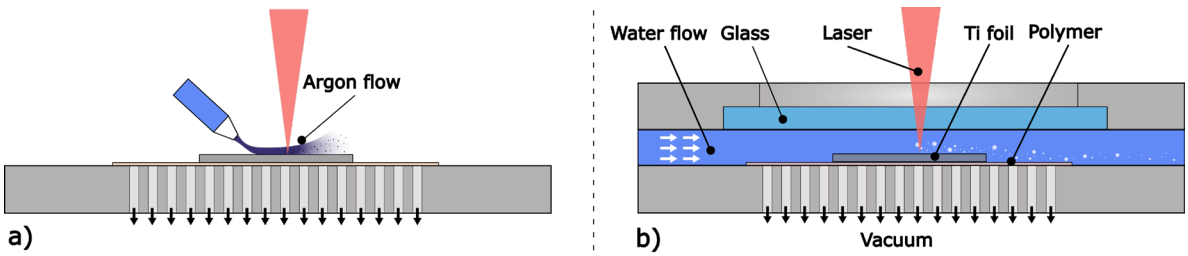

Fig. 1. (a) processing under a constant flow of argon; b) Chamber for processing in flowing liquid environment. The titanium foil sticks on a polymer and is held in place by a vacuum for both processes

3. Results

3.1. Ablation depth for processing in Argon

Figure 2 shows the ablation depth as a function of fluence at different scanning speeds. As expected, the ablation depth increases with higher fluences and lower scanning speed. While figure 2a shows a constant increase in ablation depth with increasing power figure 2b shows unexpected results for low scanning speeds that need to be closely looked at: After the ablation depth increases initially, beyond 0.6-1.2 J cm^{-2} the ablation process is highly compromised. SEM images in figure 3 reveal that ablation did occur but in addition a layer grew in the ablation area. Figure 3 also shows the existence of a gap between the layer and bulk material and only a loose connection between them. EDX measurements (figure 3) show the increased existence of oxygen.

The gap between the layer and bulk material leads to the conclusion that ablation under the layer did occur in coexistence with a layer of titanium oxides. In regard to Kiel (Kiel et al. 2019) this effect can be explained by the semi transparency of the oxide layer. While Kiel observed this behavior at yttria-stabilized zirconia ceramic the effects are expected to be comparable to TiO_2. While the titanium itself is not transparent the initial laser pulses transform the titanium to titanium oxides. As a result, the surface becomes semitransparent for the wavelength of the laser and the following laser pulses (Antończak et al. 2014). At this point the ablation threshold is not reached anymore. Reasons are expected to be defocusing effects and plasma shielding. Still, the ablation threshold is exceeded again underneath the oxide layer, indicating self-focusing in the oxide. (Tabie et al. 2019) found the threshold for self-focusing in titanium dioxide to be at 0.1 MW, which reinforces the assumption that self-focusing occurred in this process.

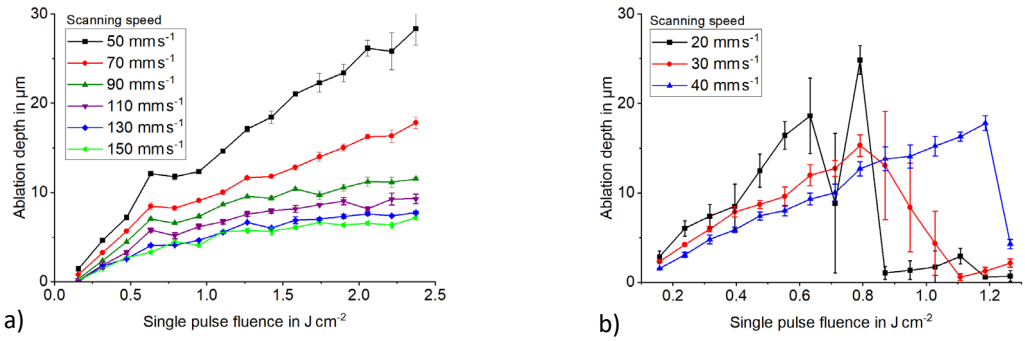

Fig. 2. Ablation depth in argon as a function of single pulse fluence and different scanning speeds. (a) The ablation depth rises with increasing fluence and decreasing scanning speed between 50 mm s^{-1} and 150 mm s^{-1}; (b) for scanning speeds between 20 mm s^{-1} and 40 mm s^{-1} the ablation is highly compromised after an initial increase.

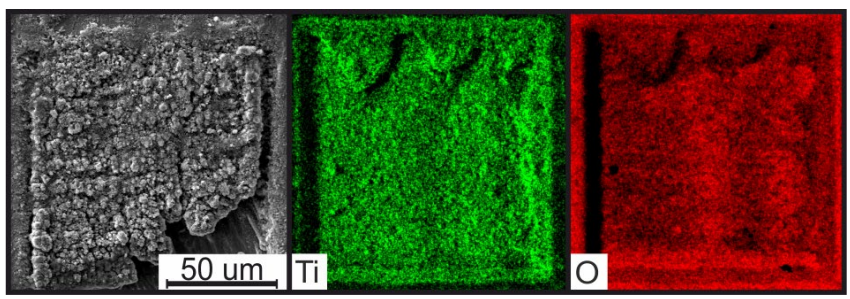

Fig. 3.: SEM image of the area processed in argon environment. An oxide layer grew, which is only loosely connected to the bulk material. Ti) EDX measurements show a uniform distribution of titanium and in O) also uniformly distributed oxygen.

3.2. Ablation depth for processing in water

As mentioned above, the ablation parameters for the experiments in liquid environment had to be adjusted compared to processing in gaseous environment, to derive comparable results. As seen in figure 2 and figure 4 the ablation depth in gaseous environment is much higher than in water when using comparable laser parameters. Thus, the energy was increased for processing in water. The results also show an increasing ablation depth with an increasing energy density, but the rise of ablation depth not constant. After the ablation depth reaches its first maximum at around 0.3 Jcm^{-1} it quickly declines before rising again above 2 J cm^{-1}.

After the first maximum the ablation rate rises much slower before reaching a plateau starting at around 5 J cm^{-1}. The already mentioned self-focusing is not expected to be responsible alone for this nonlinearity and only to play a minor role in this behavior. A much larger impact can be expected from the liquid's reaction to the high energy input: Cavitation bubbles, long lasting bubbles and plasma plumes interact in the ablation area, leading to disturbances of the laser beam. Those disturbances have been subject to many experimental studies (Butkus et al. 2019; Kanitz et al. 2019). The bubbles not only interact with the laser but also affect the plasma. For example, can the confinement of the ablation plume lead to an increasingly dense plasma, which in turn can lead to thermal accumulation in the ablation zone and changing ablation rates.

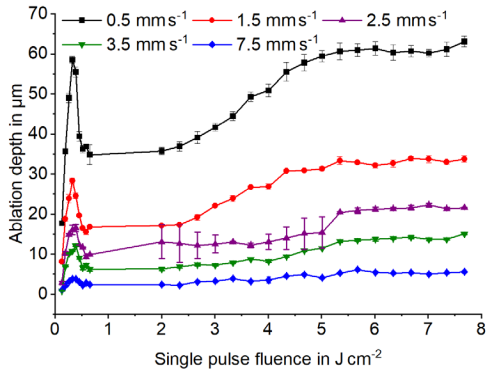

Fig. 4.: Ablation depth for processing in water as a function of fluence. A selection of different flow rates of water is shown. The first maximum in ablation depth at 2 J cm^{-1} is followed by a decline and afterwards an increase in ablation depth, reaching a plateau at around 5 J cm^{-1}.

3.3. Surface properties

The surface roughness is investigated as a quality factor and indicator for effects taking place during the ablation. As shown in figure 5 a mayor difference between the two media and process parameters can be observed. While an increasing number of ablation steps n leads to an increase in surface roughness for both media the difference between the all in all roughness is remarkable. While low fluences lead to low surface roughness in argon environment it increases quickly with higher fluences. Different to this behavior the surface roughness starts at slightly higher values for processing in water. In contrary to processing in argon environment it does not further increase with a higher number of scanning passes. Instead, it stays almost constant for a single pass. For further scanning passes it starts at higher values and decreases slightly with increasing fluences.

The surface roughness indicates that the surface structure changes with the different processing parameters. SEM images in figure 6 confirm these differences ranging from random formations to self-organized structures. Laser induced periodic surface structures (LIPSS) can be found for processing in argon at low fluences near the ablation threshold while larger periodic structures are found for processing in liquid with both lower and higher fluences. How the structures in water are formed is not investigated in this study. Taking a closer look on cavitation bubble dynamics could be a promising path to follow.

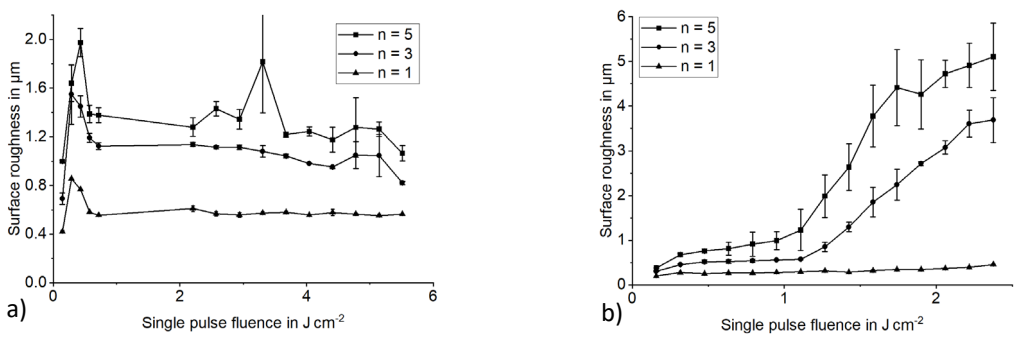

Fig. 5.: Surface Roughness for the ablation process in water a) and argon b). The roughness was evaluated for different numbers of scanning passes n.

Examining the surface with EDX a distribution of oxygen was detected that implies the occurrence of TiO_x for both processing in liquid and gaseous environment. Determining the composition of the oxides was then conducted by Ramanspectroscopy to specify the type of the oxides. A selection of spectra in figure 7 show that TiO_2 can be detected after processing in argon with characteristic peaks at 447 cm^{-1} and 612 cm^{-1}. In comparison the process in water only shows an indistinguishable signal, which does not show any significant peaks.

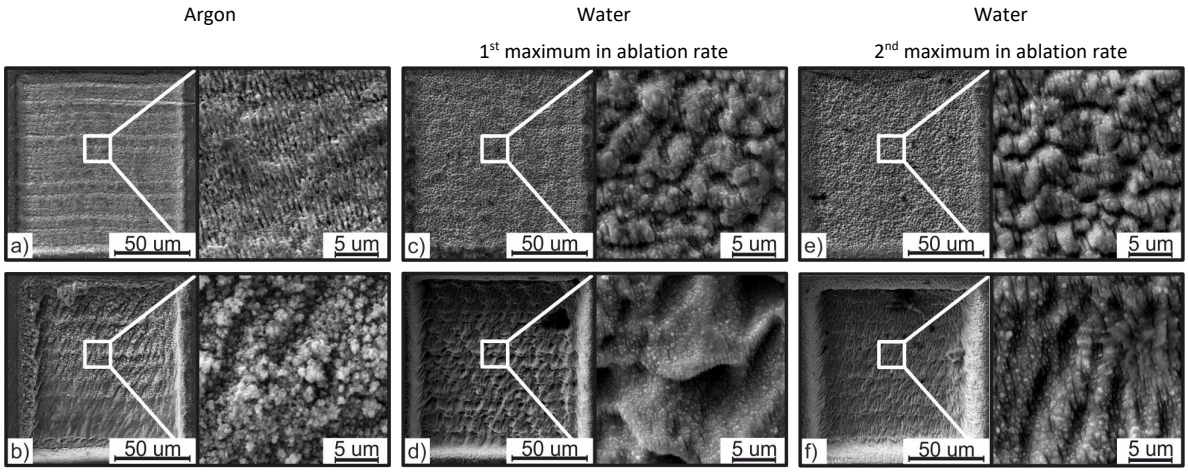

Fig. 6.: SEM image of the surface structure for processing in argon (a-b) and water (c-f) environment. Processing in argon was performed close to the ablation rate while processing in water was performed at the first maximum in ablation rate shown in figure 4 and the second maximum / plateau, also shown in figure 4. While the first row (a, c, e) shows a field which was only processed once the second row shows the surface after being processed several times.

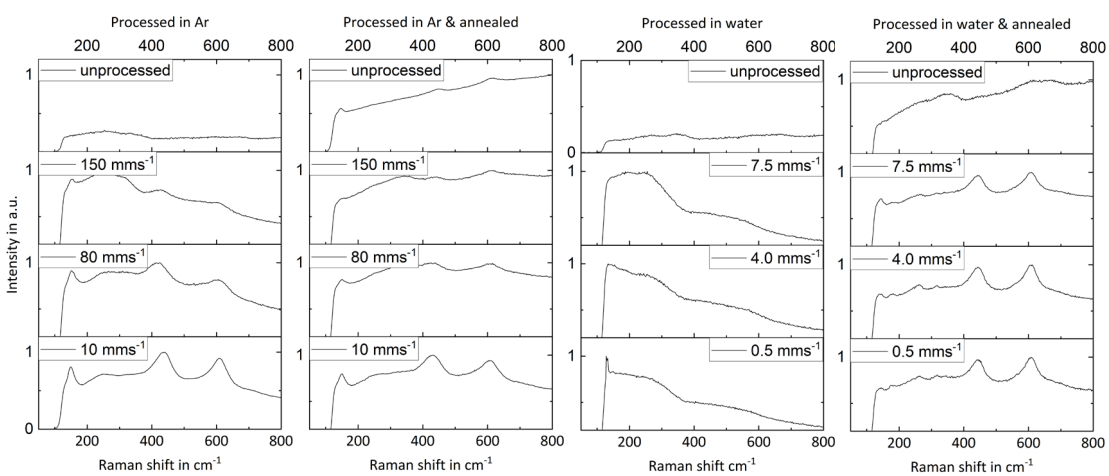

Fig. 7.: Raman Measurements for processed titanium in water and argon. Both samples were investigated before and after annealing for 1h at 500°C. While significant rutile peaks can be observed for argon before and after annealing, processing in water only shows TiO_2 peaks after annealing.

As shown by (Hoppius et al. 2018) the Raman activity is dependent on the oxides' structure. In accordance with (Wang et al. 2011) the foils were annealed in a vacuum oven at 500°C for 1 hour to achieve a crystalline

structure of the oxides. After annealing the samples that were processed in water show rutile TiO_2 peaks, too. Further titanium oxides and titanium sub oxides (Ti_nO_{2n-1}) are expected to occur in small numbers but were not proven in our measurements. As a result, it is shown that the oxides' structures differ for processing in water and in argon, while the chemical composition remains the same.

4. Conclusion

The results of laser ablation in water and argon environment were compared using titanium foils of 125 µm thickness. During this study the formation of free-floating oxide layers were observed while using high energy input in argon environment. While this effect could be possibly reduced by a completely oxygen-free environment it shows an effect that was further observed. The loose connection of the oxide layer to the bulk material indicates a continuing ablation process under the existing oxide layer. A possible explanation might be found in defocusing effects of the laser beam above the oxides surface and again self-focusing while propagating through the oxide.

For parameters which did not lead to a growth of such an oxide layer the results were compared to processing in water. The development of the ablation rate follows different characteristics for changing the energy input. While the ablation rate rises constantly in argon for increasing fluences it behaves non-linearly for processing in water. After the ablation rate reaches a maximum at around 0.3 Jcm^{-1} it undergoes an abrupt decrease before it rises again starting at around 2 Jcm^{-1}, reaching a plateau at around 5 Jcm^{-1}. Reasons for this non-linearity might be found in plasma shielding and disturbance of the process by the liquid's reaction to the high energy input by the laser beam resulting in bubble formations.

While the process is slower when using water as surrounding medium, the surface characteristics make processing in water favorable to processing in gas in terms of surface quality. For repetitive ablation passes the surface roughness decreases slightly when processing in water, while in argon a drastic increase can be observed. Raman measurements show the occurrence of TiO_2 on the surface for both processing in water and argon. Although both surfaces show TiO_2 the structure of the oxides differ. The Raman measurements indicate that processing in water leads to amorphous oxides while processing in argon environment leads to rutile TiO_2.

Acknowledgements

This project was supported by the Federal Ministry of Economic Affairs and Climate Action (IGF project no.: 21971 N)

References

Antończak AJ, Stępak B, Kozioł PE, Abramski KM, 2014. The influence of process parameters on the laser-induced coloring of titanium. Applied Physics A, 115 (3), 1003–1013.

Barthels T, Reininghaus M, 2018 - 2018. High precision ultrashort pulsed laser drilling of thin metal foils by means of multibeam processing. In: Dudley A, Laskin AV (eds.). Laser Beam Shaping XVIII, 19.08.2018 - 23.08.2018. SPIE, p. 10.

Bauer F, Michalowski A, Kiedrowski T, Nolte S, 2015. Heat accumulation in ultra-short pulsed scanning laser ablation of metals. Optics express, 23 (2), 1035–1043.

Butkus S, Gaižauskas E, Mačernytė L, Jukna V, Paipulas D, Sirutkaitis V, 2019. Femtosecond Beam Transformation Effects in Water, Enabling Increased Throughput Micromachining in Transparent Materials. Applied Sciences, 9 (12), 2405.

Hoppius JS, Bialuschewski D, Mathur S, Ostendorf A, Gurevich EL, 2018. Femtosecond laser crystallization of amorphous titanium oxide thin films. Applied Physics Letters, 113 (7).

Kanitz A, Kalus M-R, Gurevich EL, Ostendorf A, Barcikowski S, Amans D, 2019. Review on experimental and theoretical investigations of the early stage, femtoseconds to microseconds processes during laser ablation in liquid-phase for the synthesis of colloidal nanoparticles. Plasma Sources Science and Technology, 28 (10), 103001.

Kiel F, Bulgakova NM, Ostendorf A, Gurevich EL, 2019. Selective Delamination upon Femtosecond Laser Ablation of Ceramic Surfaces. Physical Review Applied, 11 (2).

Liu JM, 1982. Simple technique for measurements of pulsed Gaussian-beam spot sizes. Optics letters, 7 (5), 196–198.

Tabie VM, Koranteng MO, Yunus A, Kuuyine F, 2019. Water-Jet Guided Laser Cutting Technology- an Overview. Lasers in Manufacturing and Materials Processing, 6 (2), 189–203.

Vorobyev AY, Kuzmichev VM, Kokody NG, Kohns P, Dai J, Guo C, 2006. Residual thermal effects in Al following single ns- and fs-laser pulse ablation. Applied Physics A, 82 (2), 357–362.

Wang X, Shen J, Pan Q, 2011. Raman spectroscopy of sol-gel derived titanium oxide thin films. Journal of Raman Spectroscopy, 42 (7), 1578–1582.